

Protective effects of lipoic acid on chrysene-induced toxicity on Müller cells in vitro

Saffar Mansoor,¹ Navin Gupta,¹ Georgia Luczy-Bachman,² G. Astrid Limb,³ Baruch D. Kuppermann,¹ M. Cristina Kenney¹

¹From the Gavin Herbert Eye Institute, School of Medicine, University of California, Irvine, CA; ²Department of Pediatrics, Clinical Translational Science Center, University of California, Irvine, CA; ³Department of Ocular Biology and Therapeutics, UCL, Institute of Ophthalmology, London, United Kingdom

Purpose: This study evaluates the toxic effects of chrysene (a component from cigarette smoke) on Müller cells (MIO-M1) in vitro and investigates whether the inhibitor lipoic acid can reverse the chrysene-induced toxic effects.

Methods: MIO-M1 cells were exposed to varying concentrations of chrysene with or without lipoic acid. Cell viability was measured by a trypan blue dye exclusion assay. Caspase-3/7 activity was measured by a fluorochrome assay. Lactate dehydrogenase (LDH) release was quantified by an LDH assay. The production of reactive oxygen/nitrogen species (ROS/RNS) was measured with a 2',7'-dichlorodihydrofluorescein diacetate dye assay. Mitochondrial membrane potential ($\Delta\Psi_m$) was measured using the JC-1 assay. Intracellular ATP content was determined by the ATPLite kit.

Results: MIO-M1 cells showed significantly decreased cell viability, increased caspase-3/7 activity, LDH release at the highest chrysene concentration, elevated ROS/RNS levels, decreased $\Delta\Psi_m$ value, and decreased intracellular ATP content after exposure to 300, 500, and 1,000 μM chrysene compared with the control. Pretreatment with 80 μM lipoic acid reversed loss of cell viability in 500- μM -chrysene-treated cultures (24.7%, $p < 0.001$). Similarly, pretreatment with 80 μM lipoic acid before chrysene resulted in decreased caspase-3/7 activities (75.7%, $p < 0.001$), decreased ROS/RNS levels (80.02%, $p < 0.001$), increased $\Delta\Psi_m$ values (86%, $p < 0.001$), and increased ATP levels (40.5%, $p < 0.001$) compared to 500- μM -chrysene-treated cultures.

Conclusions: Chrysene, a component of cigarette smoke, can diminish cell viability in MIO-M1 cells in vitro by apoptosis at the lower concentrations of Chrysene (300 and 500 μM) and necrosis at the highest concentration. Moreover, mitochondrial function was particularly altered. However, lipoic acid can partially reverse the cytotoxic effect of chrysene. Lipoic acid administration may reduce or prevent Müller cell degeneration in retinal degenerative disorders.

Age-related macular degeneration (AMD) is the leading cause of vision loss in the aging population in the Western world [1]. The prevalence of the disease is expected to increase in the coming years as people live longer, and this calls for a better understanding of the mechanisms involved in AMD. The early clinical presentation of the disease is altered pigmentation and/or yellowish subretinal deposits known as drusen in the macula. Over time, drusen may become confluent and lead to degeneration of retinal pigment epithelium (RPE) cells and/or photoreceptors (dry form). In the wet form of AMD, growth of choroidal blood vessels into the retina occurs, which is referred to as choroidal neovascularization (CNV). Both forms of AMD can have damaging effects on central visual function [2].

The pathogenesis of AMD is still unknown, but multiple studies have linked cigarette smoking to an increased risk

of AMD development [3-5]. A twofold to fourfold increase risk of AMD has been found in smokers as compared with nonsmokers [4-6]. Cigarette smoking has been associated with the development of both the wet form of AMD as suggested in the macular photocoagulation study of 1986 [7] as well as the late, dry form or geographic atrophy [2,6,8].

Although cigarette smoke contains over 4,000 chemicals, polycyclic aromatic hydrocarbons (PAH) are the most toxic substances known to be present in cigarette smoke. Chrysene is one of the PAHs found in cigarette smoke. Each cigarette delivers approximately 60 ng of chrysene (Speclab) [9]. However, it is difficult to ascertain the quantitative level of chrysene because of variability in smoking devices, such as cigarettes (which come in various sizes), cigars, pipes stuffed with tobacco or hookas/beedies (raw tobacco) used in old world cultures, frequency of smoking, average inhalation, the concentration ultimately inhaled, amount of chrysene (from smoke) reaching systemic circulation, and the quantity cross through the blood-retinal barrier to reach into the retina. In addition, chrysene is a soil and water contaminant and also occurs as a ubiquitous environmental pollutant from smoked

Correspondence to: M. Cristina Kenney, Gavin Herbert Eye Institute, Ophthalmology Research Laboratory, University of California Irvine, Hewitt Hall, Room 2028, 843 Health Science Rd., Irvine, CA 92697; Phone: (949) 824-7603; FAX: (949) 824-9626, email: mkenney@uci.edu

foods, coal gasification, road and roof tarring, incinerators, and aluminum production (IARC) [10,11].

In vitro and in vivo studies have shown that PAH can have chemical effects via formation of DNA adducts, which lead to cellular proliferation [12-14]. Chrysene or its derivative have mutagenic, carcinogenic [15], and genotoxic [16,17] effects in animal and cell culture studies. Chrysene caused alteration in immune function and CYP450 activity in adult male deer mice (*Peromyscus maniculatus*) [18]. In addition, chrysene showed toxic effects in rat liver epithelial cells [19] and in marine organisms [20].

In smokers, retinal tissues that can be damaged secondary to degeneration of RPE cells and Bruch's membrane are the neurosensory cells (photoreceptors) and supportive glial cells [21,22]. Postmortem eyes of patients with AMD have shown death of photoreceptors, inner nuclear layer, and RPE cells [23]. As of yet, there are few studies on the effects of chrysene in human retinal cells. Our overall goal is to investigate the pathophysiology of cigarette smoke in AMD. Investigators have examined other smoking toxicants, such as benzo-a-pyrene (BeP) [24,25] and nicotine [26] with and without various inhibitors that can reverse their toxic effects. Nicotine treatment showed a differential response of cells ranging from not being affected at all (ARPE-19 cells) to loss of cell viability via necrosis (human microvascular endothelial cells [HMVEC]) or cell damage through an oxidant pathway (R28 cells) [26]. Jia et al. reported that acrolein, a toxicant in cigarette smoke, causes oxidative damage and mitochondrial dysfunction in RPE cells which was exposed to the protective agent alpha-lipoic acid (LA) [27]. These findings underscore the challenges in developing effective inhibitor therapies to reverse smoking-related cell damage. We are now expanding our studies to include human retinal glial cells and their response to smoking-related compounds.

Inhibitors studied in our laboratory are memantine, epicatechin, resveratrol, and genistein, all of which showed significant inhibitory effects against smoking constituents and other toxins, such as ketocholesterol [25,26,28]. Recently, LA has shown great promise in protecting cells against various toxicants, including those from smoke [29,30]. LA is a sulfur-containing compound found naturally in plants and animals. Dihydrolipoic acid is the reduced form, which is the form that exists intracellularly. It is present in mitochondria as an essential cofactor for pyruvate dehydrogenase and α -ketoglutarate dehydrogenase [31]. LA can scavenge hydroxyl radicals, singlet oxygen, peroxyxynitrite, and nitric oxide [31,32]. In addition it can chelate several transition metal ions [31,33], has antioxidant properties, and is reported to provide protection against oxidative injury in various

disease process, including neurodegenerative disorders and diabetic syndrome [34,35]. This study investigates whether chrysene causes injury, especially mitochondrial dysfunction, to Müller cells and whether LA would protect it from chrysene-mediated injury and mitochondrial dysfunction.

METHODS

Cell culture and treatments: The human Müller cell line (MIO-M1) [36] was grown in Dulbecco's modified Eagle medium (D-MEM; 1 \times) high glucose SKU#10569-044 (GlutaMAX-1 medium substituted on a molar equivalent basis for L-glutamine, 4500 mg/l D-glucose, 110 mg/l sodium pyruvate, 1 \times penicillin/streptomycin, and 10% fetal bovine serum). MIO-M1 cells that were used for these series of experiments were of passage 26 to 30. Cells were plated in 6-, 96-, or 24-well plates (Becton Dickinson Labware, Franklin Lakes, NJ) for cell viability (5×10^5 cells/well), caspase-3/7 activity (1.2×10^5 cells/well), lactate dehydrogenase (LDH; 1.2×10^5 cells/well), mitochondrial membrane potential (1.2×10^5 cells/well), reactive oxygen/nitrogen species (ROS/RNS) detection (1.2×10^5 cells/well), and ATP measurement (1.0×10^5 cells/well) assays and were incubated at 37 °C in 5% CO₂ until monolayer confluence was achieved. Cells were incubated further in serum-free culture medium for 24 h to make them relatively nonproliferating. This was done to simulate the condition of natural human retina in which Müller cells remain in a nonproliferating phase and are not exposed to the circulation because of the blood-retinal barrier [24].

Exposure to chrysene: Chrysene was procured from Sigma Aldrich Inc. (St Louis, MO), and the stock solution (100 mM chrysene) was prepared by solubilizing 0.0228 gm of chrysene in 1 ml of dimethyl sulfoxide (DMSO). Thereafter, different dilutions were prepared by adding to the culture media. Cells were treated with 1,000 μ M, 500 μ M, 300 μ M, and 100 μ M chrysene for 24 h. Some other concentrations of chrysene (5, 10, 20, 30, and 40 μ M) were also used to treat cells for 24 h or 7 days. Cells with equivalent DMSO (without chrysene) served as control cultures.

Cell viability studies: MIO-M1 cells were treated with chrysene in three different ways: (a) acute exposure with 10, 20, 30, and 40 μ M chrysene for 24 h, (b) chronic exposure with 5, 10, 20, and 30 μ M chrysene for 7 days, and (c) treatment with 100, 300, 500, and 1,000 μ M chrysene for 24 h. The cell viability (CV) assay was performed as described by Narayanan et al. [37]. Cells were harvested from the six-well plates by treatment with 0.2% trypsin-EDTA and then incubated at 37 °C for 5 min. The cells were centrifuged at 3920 \times g for 5 min and resuspended in 1 ml of culture medium. CV was

analyzed by a Vi-cell series cell viability analyzer (Beckman Coulter Inc., Fullerton, CA). The analyzer performs an automated trypan blue dye-exclusion assay and gives the percentage of viable cells.

Inhibition studies with lipoic acid: To examine inhibitory effects on loss of CV, cells were pretreated for 6 h with different concentrations of R-alpha-LA (Sigma Aldrich Inc.) and then replaced with chrysene+LA. LA was dissolved in distilled water and prepared as 10, 20, 40, 80, or 100 μ M in culture media. Chrysene was added to the pretreated cells, which were then cultured overnight and analyzed for CV. The higher percentage of viable cells in the pretreated cultures indicated a greater inhibitory effect. Therefore, the optimum inhibitory effect of LA at a particular concentration was determined on the basis of percentage viable cells.

Caspase-3/7 assays: To verify apoptosis as a cell death mechanism, caspase-3/7 activity was detected using fluorescent-labeled inhibitor of caspases apoptosis (FLICA) detection kits (Immunochemistry Technologies LLC, Bloomington, MN). The FLICA reagent has an optimal excitation range from 488 to 492 nm and an emission range from 515 to 535 nm. Caspase-3/7 activities were measured using a fluorescence image scanning unit instrument (FMBIO III; Hitachi, Yokohama, Japan), which quantified apoptosis as the amount of green fluorescence emitted from FLICA probes bound to caspase-3/7.

At the designated time period, the wells were rinsed briefly with fresh culture media, replaced with 300 μ l/well of 1 \times FLICA solution in culture media, and incubated at 37 $^{\circ}$ C for 1 h under 5% CO₂. Cells were washed with PBS (8g NaCl, 0.2g KCl, 1.15 g Na₂HPO₄, 0.2g KH₂PO₄ dissolved in one liter dionized water). Non-apoptotic cells appeared unstained, while cells undergoing apoptosis fluoresced brightly. The following controls were included: untreated MIO-M1 cells without FLICA to exclude auto fluorescence from MIO-M1 cells; untreated MIO-M1 cells with FLICA for comparison of caspase activity of treated cells; tissue culture plate wells without cells with buffer alone to represent the background level; tissue culture plate wells without cells with buffer and DMSO to exclude the cross-reaction of FLICA with DMSO and culture media; MIO-M1 cells with DMSO and FLICA to account for any cross-fluorescence between untreated cells and DMSO. Quantitative calculations of caspase activities were performed with an FMBIO III (Hitachi). The caspase activity was measured as the average signal intensity of the fluorescence of the pixels in a designated spot (mean signal intensity [msi]).

DNA fragmentation assay: MIO-M1 cells (5×10^5) were plated overnight in six-well plates and then incubated for

another 24 h with different concentrations of chrysene. DNA was extracted (QIAamp DNA Micro kit; Qiagen, Hilden, Germany) according to the manufacturer's instructions. Briefly, the cells in the experiment were first lysed. The lysate was then transferred onto the kit columns. As the columns were centrifuged, the DNA present in the lysate was adsorbed onto-the silica gel membrane. While DNA remained bound to this silica membrane, the columns were made to get rid of contaminants by washing away with buffers AW1 and AW2. DNA was then eluted from the columns using distilled water. Samples were separated by electrophoresis on 3% agarose gels and were stained with 5% ethidium bromide. 100 bp DNA step ladder marker from Promega was used, and images were captured with an FMBIO III (Hitachi).

Lactate dehydrogenase cytotoxicity assay: LDH is a cytosolic enzyme present in all mammalian cells and is released following damage of the plasma membrane. Therefore, LDH is the marker of cell death, and this assay is a test for cytotoxicity in vitro. The activity of released LDH in culture supernatant was measured with a commercial LDH-Cytotoxicity Assay Kit II (BioVision Research Products, Mountain View, CA). The basis of this kit is a coupled enzymatic reaction in which LDH present within the sample catalyzes the conversion of lactate into pyruvate with the concomitant formation of nicotinamide adenine dinucleotide (NADH) from NAD⁺. The NADH is then used as a cofactor in the conversion of the tetrazolium salt, 2-p-iodophenyl-3-p-nitrophenyl tetrazolium chloride, into a red formazan product; this second reaction is catalyzed by the enzyme diaphorase, which is present within the assay substrate mixture. The absorbance of the formazan product is measured at 490 nm. Formazan concentrations are directly proportional to the concentration of LDH in the sample.

The LDH cytotoxicity assay was performed following the supplier's protocol. Briefly, MIO-M1 cells were plated with 100 μ l culture medium in each well in 96-well plates (in triplicate). There were untreated controls and background controls having the same volume of culture medium per well with and without cells, respectively. After chrysene treatment, the 96-well plate was shaken gently for even distribution of LDH in the culture medium. The cells were centrifuged at $58,800 \times g$ for 10 min to precipitate the cells. Then 50 μ l of supernatant was transferred into a new 96-well plate, which was treated with 100 μ l/well of LDH reaction mixture (LDH reaction mixture was prepared by mixing the water-soluble terazolium (WST) substrate mix with LDH assay buffer). After 30-min incubation at room temperature, the LDH activity was quantified as absorbance values (optical density [OD]) at 490 nm by a multiwell spectrophotometer

(Victor 2 microplate reader; Perkin Elmer, Wellesley, MA). The plate was read at multiple time points until consistent readings were obtained. LDH activity in each cell lysate was expressed as percent increase in LDH activity with respect to equivalent DMSO control.

Detection of reactive oxygen/nitrogen species production: ROS/RNS production was measured with the fluorescent dye 2',7'-dichlorodihydrofluorescein diacetate assay (H₂DCFDA; Invitrogen, Molecular Probes, CA) [38], which detects hydrogen peroxide, peroxy radicals, and peroxy-nitrite anions. The cells were washed with sterile PBS and incubated with 500 μ l of 10 μ M H₂DCFDA for 30 min at 37 °C and again washed with PBS. The H₂DCFDA (10 μ M) was prepared by adding 2 μ l of 5 mM (H₂DCFDA) stock/ml in serum-free culture media. The 5 mM H₂DCFDA stock solution was prepared fresh by mixing 0.005 g of H₂DCFDA in 2.05 ml of DMSO. ROS/RNS production was measured with the scanning unit (excitation 488 nm, emission 520 nm; FMBIO III; Hitachi).

Mitochondrial membrane potential assay: Loss of the $\Delta\Psi_m$ is a hallmark for cellular apoptosis and was measured using the JC-1 mitochondrial membrane potential detection kit (Biotium, Hayward, CA). JC-1 contains a cationic dye (5,5',6,6'-tetrachloro-1,1',3,3'-tetraethyl-benzimidazolyl-carbocyanine-iodide) that fluoresces red in the mitochondria of live cells. In dead cells the mitochondrial membrane potential collapses and the cationic dye remains in the cytoplasm and fluoresces green. Typically, the ratio of red to green fluorescence is higher in healthy cells and comparatively lower in apoptotic cells.

The JC-1 assay was conducted as per the supplier's instructions. Briefly, at the end of the 24 h of chrysene with or without lipoic acid exposure, the cells were rinsed with fresh media and incubated for 15 min with 500 μ l/well of JC-1 reagent in culture media. Images were captured using an FMBIO III instrument (Hitachi) and the red/green fluorescence ratios were calculated.

Measurement of intracellular ATP: Intracellular ATP level was measured using the luminescence ATP detection assay (ATPlite PerkinElmer Inc., Waltham, MA) as per the supplier's instruction. ATPlite assay is based on production of light caused by the reaction of ATP with added luciferase and D-luciferin (just like the firefly luciferase). The emitted light is proportional to the ATP concentration. Cells were first plated in the 96-well culture plate. Cell lysis solution was added to the wells to lyse the cells and release the ATP. Exposure time was 5 min. Luciferase and D-luciferin is then added to it. Exposure time was 5 min. Then the plate was

dark adapted for 10 min. The luminescence is then measured with the reader.

ATP is a marker for cell viability. Its concentration in the cell declines rapidly when the cell dies either due to necrosis or apoptosis. This assay is based on light production caused by the reaction of ATP with added luciferase and D-luciferin. The emitted light is proportional to the ATP concentration within certain limits.

Briefly, MIO-M1 cells were first plated on 96-well plates (100,000 cells per 100 μ l culture media/well) and were incubated overnight. They were pretreated with different concentrations of chrysene. To each well, 50 μ l of mammalian cell lysis solution was added, which opens up the cells allowing the intracellular ATP to be released. To each well, 50 μ l of ATPlite buffer (HEPES (4-(2-hydroxyethyl)-1-piperazineethanesulfonic acid) is a zwitterionic organic chemical buffering agent) was added, which contained luciferase and D-luciferin. The microplate was then shaken for 5 min at 6860 \times g. The plate was covered with an adhesive seal, dark-adapted for 10 min, and luminescence was measurement using a luminescence microplate reader (BioTek Instrument, Inc., Winooski, VT). The ATP standard curve was made by plotting signal verses ATP concentrations. The signal for the unknown sample was obtained by using a linear regression equation.

Statistical analysis: Data were subjected to statistical analysis by ANOVA (Prism, version 3.0; GraphPad Software Inc., San Diego, CA). Newman-Keuls multiple-comparison test was done to compare the data within each experiment. A value of $p < 0.05$ was considered statistically significant. Error bars in the graphs represent the standard error of the mean with experiments performed in triplicate.

RESULTS

Cell viability studies: MIO-M1 cells exposed to chrysene 20, 30, 40, and 80 μ M for 24 h did not show toxic effects on cells (Figure 1A). However, cells treated with 30 μ M chrysene for 7 days (chronic exposure) showed significantly reduced cell viability (91.85 \pm 0.6%, $p < 0.05$) as compared to controls (95.45 \pm 0.55%); treatment with 5, 10, and 20 μ M chrysene for 1 week did not affect cell viability on MIO-M1 cells (Figure 1B). MIO-M1 cells showed loss of CV after exposure to higher concentrations of chrysene for 24 h (Figure 1C). The mean percentage of viable cells was 53.1 \pm 2.1 ($p < 0.001$), 66.1 \pm 1.9 ($p < 0.001$), and 90.65 \pm 0.55 ($p < 0.05$) at 1,000, 500, and 300 μ M chrysene, respectively, compared to DMSO-treated controls. At 100 μ M chrysene, CV was 96.3 \pm 0.5 ($p > 0.05$). The mean percentages of cell viability of DMSO-treated equivalent cultures of 1,000 (95.56 \pm 0.5),

500 (96.15±0.65), 300 (96.45±0.6), and 100 (96.75±0.8) μM were similar to those of the untreated MIO-M1 cultures (98.5±1). Cell death induced by 1,000 μM chrysenes was not protected by pretreatment with LA (40, 80, and 100 μM) at any of the studied concentrations (Figure 1D). The optimum increase in mean percentage of CV due to pretreatment with LA 80 μM was 4.85% (55.75±1.25, p>0.05) as compared to 1,000 μM chrysenes alone (50.9±0.89). However, in the MIO-M1 cells exposed to 500 μM chrysenes, pretreatment with 80 μM LA significantly increased the mean percentage of CV. The increase in mean percentage of CV was 24.7 (88.2±1.5, p<0.001) as compared to 500-μM-chrysenes-treated cultures (63.5±2). Therefore, in further experiments cells were pretreated with 80 μM LA to examine the pathways for protective effects.

Caspase-3/7 activity: Caspase-3/7 activity in MIO-M1 cells increased significantly after treatment with chrysenes for 24 h (Figure 2A). Cells treated with 1,000, 500, and 300 μM chrysenes showed increase in mean fluorescence of 87% (28,066.70±698.4 msi, p<0.001), 83.7% (21,200±472.5

msi, p<0.001), and 52.5% (7666.67±296.27 msi, p<0.01), respectively. Cells treated with 100 μM chrysenes did not show a significant increase in caspase-3/7 activity (4666.667±120.7 msi, p>0.05) as compared to DMSO-treated cultures (3500.0±173.2 msi). Values for untreated and DMSO-equivalent cultures of 1,000, 500, and 300 μM were 3416.667±187.8 msi, 3663.33±144.9 msi, 3630.33±124.9 msi, and 3639±123.2 msi, respectively. Caspase-3/7 is the hallmark of apoptosis because it is the final common pathway of apoptosis. To verify apoptotic activity, DNA fragmentation analysis was performed showing DNA bands that laddered in approximately 200-bp increments, consistent with apoptosis (Figure 2B). Pretreatment with 80 μM LA resulted in 75.7% (5466.6±578.3 msi, p<0.001) reduction in caspase-3/7 activity as compared to the 500-μM-chrysenes-treated culture (22,566.67±1476.8 msi; Figure 2C).

Lactate dehydrogenase cytotoxicity assay: Treatment of MIO-M1 cells with 1,000 μM chrysenes for 24 h resulted in a 67% OD (1.95±0.04, p<0.001) increase in LDH activity as compared to the DMSO-equivalent culture (OD 0.64±0.045;

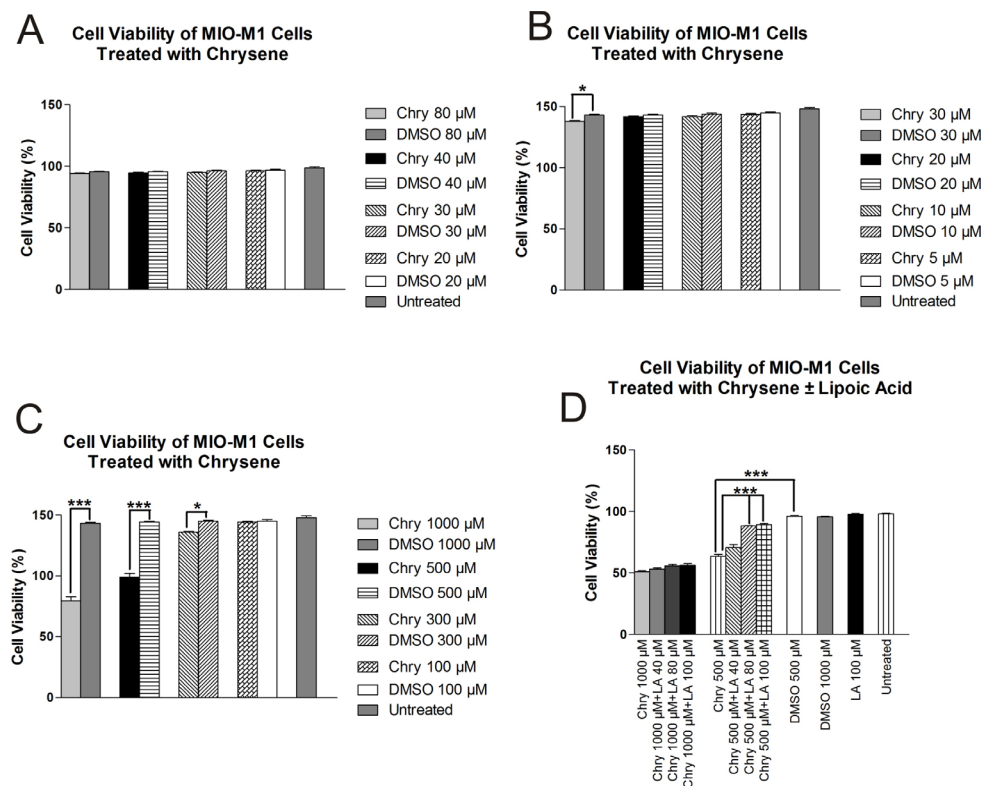
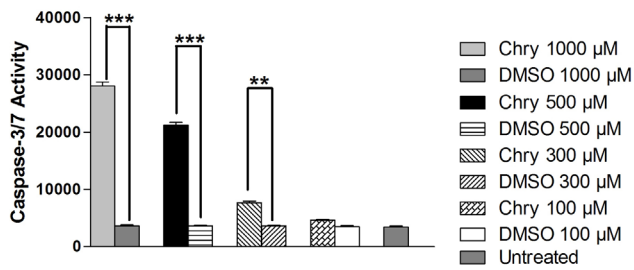


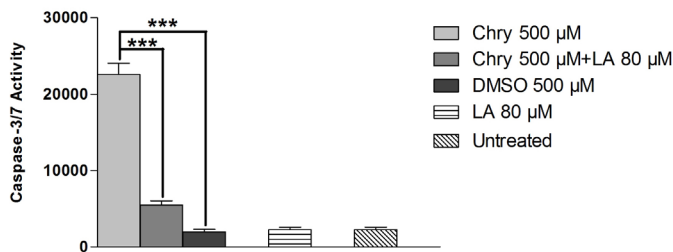
Figure 1. The effects of chrysenes on MIO-M1 cell viability. **A:** There were no changes of MIO-M1 cell viability after 24 h exposure to 20, 30, 40, and 80 μM chrysenes (Chry) compared to the dimethyl sulfoxide (DMSO)-equivalent controls. **B:** After exposure to 30 μM chrysenes for 7 days, the MIO-M1 cells showed a decrease of cell viability compared to DMSO-equivalent cells (*p<0.05). The cell viabilities in MIO-M1 cells exposed to 5, 10, and 20 μM chrysenes for 7 days were similar to DMSO-equivalent controls and untreated controls. **C:** There were significant decreases of MIO-M1 cell viabilities after 24 h treatment with 1,000 μM (***p<0.001), 500 μM (**p<0.001), and 300 μM (*p<0.05) chrysenes compared to DMSO-equivalent controls. Cultures treated with 100 μM

chrysenes showed a similar level of cell viability to DMSO-equivalent controls. **D:** Some cells were pretreatment 6 h with varying concentrations of lipoic acid (LA) and then exposed to 500 μM or 1,000 μM chrysenes (Chry +LA) for an additional 24 h. Cell viability levels were not reversed by LA pretreatment in any of the MIO-M1 cells exposed to 1,000 μM chrysenes. The loss of cell viability was reversed by pretreatment with 80 μM LA (p<0.001) and 100 μM LA (p<0.001) in the MIO-M1 cells exposed to 500 μM chrysenes. Cell viability levels were not decreased in MIO-M1 cultures treated with 1,000 μM DMSO-equivalent, 500 μM DMSO-equivalent, or by exposure to 100 μM LA alone. Assays were performed in triplicate and the experiments repeated three times. Values are mean ± standard error mean (SEM).

A Caspase-3/7 Activity of MIO-M1 Cells Treated with Chrysene



C Caspase-3/7 Activity of MIO-M1 Cells Treated with Chrysene ± Lipoic Acid



B

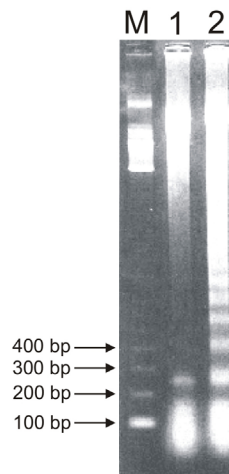


Figure 2. The effects of chrysene (Chry) treatment on caspase-3/7 activity in MIO-M1 cells. **A:** The MIO-M1 cells treated 24 h with 1,000 μM (**p<0.001), 500 μM (**p<0.001), and 300 μM (**p<0.01) chrysene showed significantly increased caspase-3/7 activities compared to dimethyl sulfoxide (DMSO)-equivalent-treated cells. The untreated cells, 100-μM-chrysene-treated cells, and equivalent-DMSO-treated cells showed similar levels of caspase-3/7 activity. **B:** Analyses of DNA fragmentation patterns for chrysene-treated MIO-M1 cells. After treatment with 100 μM chrysene (lane 2), the MIO-M1 cells showed DNA fragmentation at 200-base pair (bp) intervals compared to the untreated control cultures (lane 1) which is consistent with apoptosis. **C:** The protective effects of lipoic acid (LA) against chrysene induced

caspase-3/7 activity in MIO-M1 cells. The MIO-M1 cells pretreated 6 h with 80 μM LA followed by the addition of 500 μM chrysene (500 μM +LA 80 μM) for 24 h showed lower caspase-3/7 activity levels compared to the cells treated with 500 μM chrysene alone (**p<0.001). The untreated cells, DMSO-equivalent-treated cells (DMSO 500 μM), and cells treated with 80 μM LA alone (LA 80 μM) showed low levels of caspase-3/7 activity. Assays were performed in triplicate and the experiments repeated three times. The DNA fragmentation analyses were repeated twice. Values are mean±standard error mean (SEM). M, marker; bp, base pair.

Lactic Dehydrogenase Activity in MIO-M1 Cells Treated with Chrysene

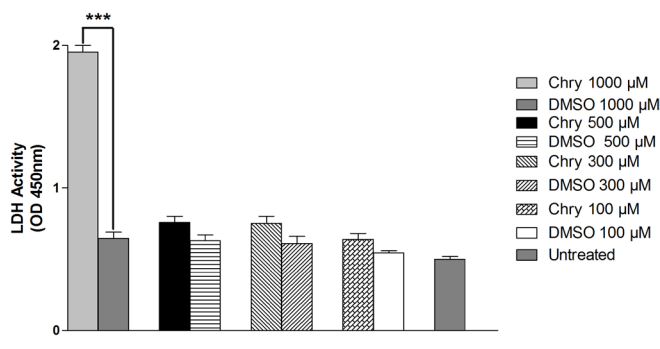


Figure 3. The effects of chrysene (Chry) on lactate dehydrogenase (LDH) levels in MIO-M1 cells. The MIO-M1 cells treated 24 h with 1,000 μM chrysene showed increased LDH levels activity (**p<0.001) compared to cells treated with the dimethyl sulfoxide (DMSO)-equivalent. The untreated cells, 500 μM-chrysene-treated cells, 300-μM-chrysene-treated cells, 100-μM-chrysene-treated cells, and their DMSO- equivalent-treated cells showed low levels of LDH. Assays were performed in triplicate and repeated three times. Assays were performed in triplicate and the experiments repeated three times. Values are mean ± standard error mean (SEM).

Figure 3). Chrysene at 500-μM (OD 0.76±0.04), 300-μM (OD 0.75±0.05), and 100-μM (OD 0.64±0.03)-treated MIO-M1 cells did not significantly increase LDH levels (p>0.05) compared to their equivalent DMSO controls (ODs 0.63±0.04,

0.61±0.05, and 0.054±0.01, respectively). The OD value for untreated MIO-M1 cells was 0.5±0.02.

Reactive oxygen/nitrogen species measurement: MIO-M1 cells treated for 24 h with 1,000, 500, and 300 μM chrysene showed significantly increased ROS/RNS levels as

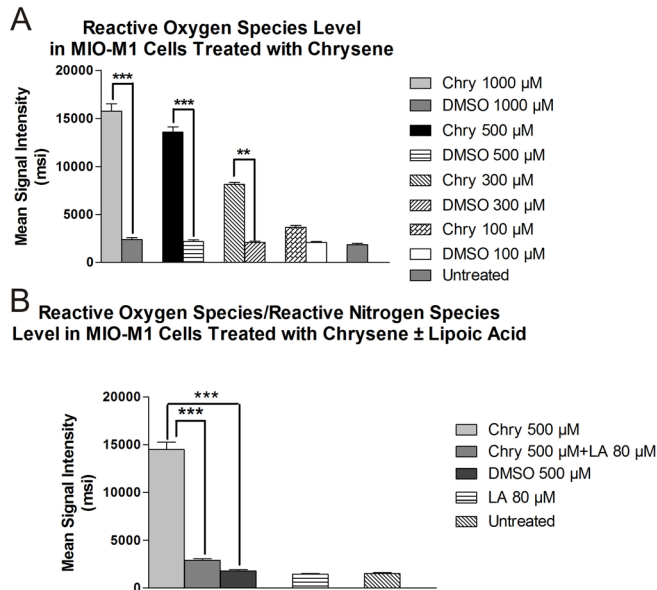


Figure 4. The effects of chrysene (Chry) on production of reactive oxygen/nitrogen species (ROS/RNS) in MIO-M1 cells. **A:** The MIO-M1 cells exposed to 1,000 μ M chrysene, 500 μ M chrysene, and 300 μ M chrysene had significantly higher ROS/RNS compared to MIO-M1 cells treated with the dimethyl sulfoxide (DMSO)-equivalent ($***p<0.001$, $***p<0.001$, $**p<0.01$, respectively). The untreated MIO-M1 cells, 100- μ M-chrysene-treated cells, and DMSO-equivalent-treated cells showed low levels of ROS/RNS production. **B:** Cells that were pretreated 24 h with 80 μ M lipoic acid (LA) and had 500 μ M chrysene added to the cultures for 24 h (Chyr 500 μ M +LA 80 μ M) showed ROS/RNS levels similar to the DMSO- equivalent-treated cultures showing a protective effect of the LA against chrysene induced ROS/RNS production. Assays were performed in triplicate and the experiments repeated three times. Values are mean \pm standard error mean (SEM).

compared to the equivalent DMSO-treated cultures as shown in Figure 4A. The mean fluorescence values were 15,766.67 \pm 721.88 msi ($p<0.001$), 13,566.67 \pm 578.31 msi ($p<0.001$), and 8166.66 \pm 176.38 msi ($p<0.01$) for 1,000, 500, and 300 μ M chrysene, respectively, as compared to the respective DMSO-treated cultures. Cells treated with 100 μ M chrysene did not show a significant increase in ROS/RNS level (3666.667 \pm 202.7 msi, $p>0.05$) as compared to DMSO-treated cultures (2066.667 \pm 120.18 msi). Values for untreated cells and DMSO-equivalent cultures of 1,000, 500, and 300 μ M were 1860 \pm 124.9, 2366.67 \pm 233.3, 2166.667 \pm 176.4, and 2086.67 \pm 135.44, respectively. Pretreatment with 80 μ M LA resulted in an 80.02% (14,466.67 \pm 785.99msi, $p<0.001$) decrease in ROS/RNS levels as compared to the 500- μ M-chrysene-treated culture (2893.333 \pm 157.19 msi; Figure 4B).

Mitochondrial membrane potential assay: MIO-M1 cells treated for 24 h with 1,000, 500, and 300 μ M chrysene showed

significantly decreased $\Delta\Psi_m$ as compared to their respective DMSO-treated cultures as shown in Figure 5A. The mean $\Delta\Psi_m$ values were 1.27 \pm 0.15 ($p<0.001$), 2.2 \pm 0.23 ($p<0.001$), and 4.23 \pm 0.20 ($p<0.05$) for 1,000, 500, and 300 μ M chrysene, respectively. Cells treated with 100 μ M chrysene did not show a significant decrease in $\Delta\Psi_m$ values (4.76 \pm 0.176, $p>0.05$) as compared to DMSO-treated cultures (5.33 \pm 0.145 msi). Values for untreated cells and DMSO-equivalent cultures of 1,000, 500, and 300 μ M were 5.5 \pm 0.12, 5.23 \pm 0.2, 5.30 \pm 0.17, and 5.31 \pm 0.19, respectively. Pretreatment with 80 μ M LA resulted in an 86% (3.84 \pm 0.05, $p<0.001$) increase in the $\Delta\Psi_m$ value as compared to the 500- μ M-chrysene-treated cultures (2.06 \pm 0.17; Figure 5B).

Intracellular ATP levels: Intracellular ATP levels in MIO-M1 cells decreased significantly after treatment for 24 h with 1,000, 500, and 300 μ M chrysene as compared to their

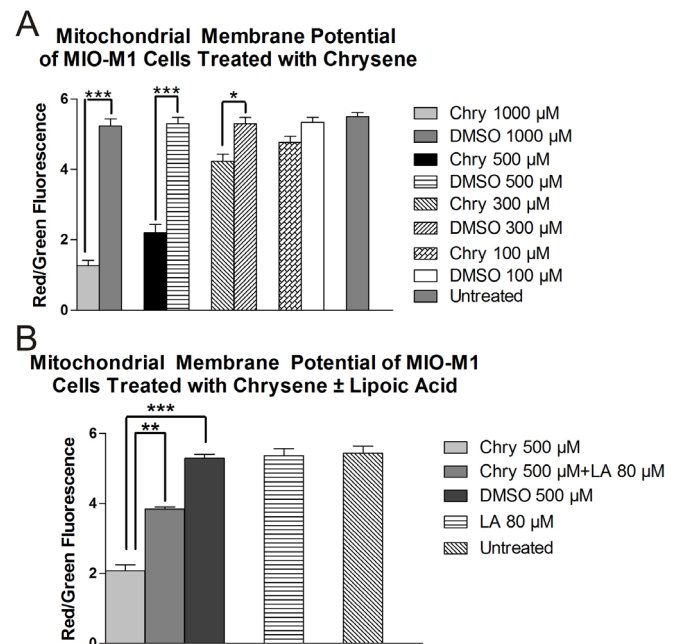


Figure 5. The effects of chrysene (Chry) on mitochondrial membrane potential ($\Delta\Psi_m$) in MIO-M1 cells. **A:** The MIO-M1 cells treated 24 h with 1,000 μ M ($***p<0.001$), 500 μ M ($***p<0.001$), and 300 μ M ($*p<0.05$) chrysene showed lower $\Delta\Psi_m$ compared to the cells treated with the dimethyl sulfoxide (DMSO)-equivalent. The 100- μ M-chrysene-treated cells and DMSO-equivalent-treated cells showed similar levels of $\Delta\Psi_m$ as the untreated cells. **B:** When the MIO-M1 cells were pretreated for 6 h with 80 μ M lipoic acid (LA) and then 500 μ M chrysene was added to the cultures for 24 h (Chyr 500 μ M +LA 80 μ M), the $\Delta\Psi_m$ was restored partially compared to the 500- μ M-chrysene-treated cells ($**p<0.01$). The 80 μ M LA did not have any affect on the $\Delta\Psi_m$ compared to untreated or DMSO-equivalent-treated cells. The assays for each concentration were run in triplicate repeats and the experiments repeated three times. Values are mean \pm standard error mean (SEM).

respective DMSO-treated cultures (Figure 6A). The mean percentage ATP levels were 41.0 ± 2.08 ($p < 0.001$), 55.3 ± 1.2 ($p < 0.001$), and 83.77 ± 2.05 ($p < 0.01$) for 1,000, 500, and 300 μM chrysene, respectively, as compared to the DMSO-treated cultures. Cells treated with 100 μM chrysene did not show a significant increase in ATP levels ($94.66 \pm 0.88\%$, $p > 0.05$) as compared to DMSO-treated cultures ($98.33 \pm 0.6\%$). Values for untreated cells and DMSO-equivalent cultures of 1,000, 500, and 300 μM were 100 ± 0 , 97 ± 1.15 , 97.83 ± 0.73 , and 98.26 ± 0.65 , respectively. Pretreatment with 80 μM LA resulted in a 40.05% (91.5 ± 1.15 , $p < 0.001$) increase in the ATP level as compared to the 500- μM -chrysene-treated cultures (51.0 ± 1.73 ; Figure 6B).

DISCUSSION

In AMD, multiple cell types within the macula can be damaged. While the primary pathology involves the RPE cells, Bruch's membrane, and the choriocapillaries [39], other cell types of the overlying neuroretina are also affected. In this study we wanted to focus on the retinal glial cells since they have an important supportive role for the health of RPE cells and the neuroretina. We used the human Müller cells as representative of the human retinal glial cells.

Human retina has three basic types of glial cells: Müller cells, astroglia, and microglia. Müller cells provide a supportive function to the neurons of the retina, including the photoreceptors, bipolar cells, and ganglion cells [40]. They also preserve the homeostasis of the retina by secreting growth factors and cytokines that maintain the outer blood-retinal barrier [41]. In AMD, these dysfunctional Müller cells are seen as accumulated lipid-bloated microglial cells in the subretinal spaces [42] and appear on funduscopy to be similar to the drusen. With loss of the RPE cell barrier, choroidal neovascularization can occur. The Müller cells may be involved indirectly in the pathology of AMD since they are supportive of the outer blood-retinal barrier, which is damaged both in the early and late stages of AMD.

Recent studies have reported the progenitor properties of Müller cells. Müller cells in isolation display features similar to retinal progenitor cells as they can renew themselves and generate all of the neuronal cell types characteristic of retina [43,44]. Following retinal degeneration, progenitor cells derived from Müller cells differentiate into several different retinal cell lineages, which can support retinal regeneration in vivo [45,46]. However, because they are limited in numbers, these new retinal cells cannot completely replace damaged tissues [45]. From the above discussion, it becomes obvious that damage to the Müller cells can have a dramatic impact,

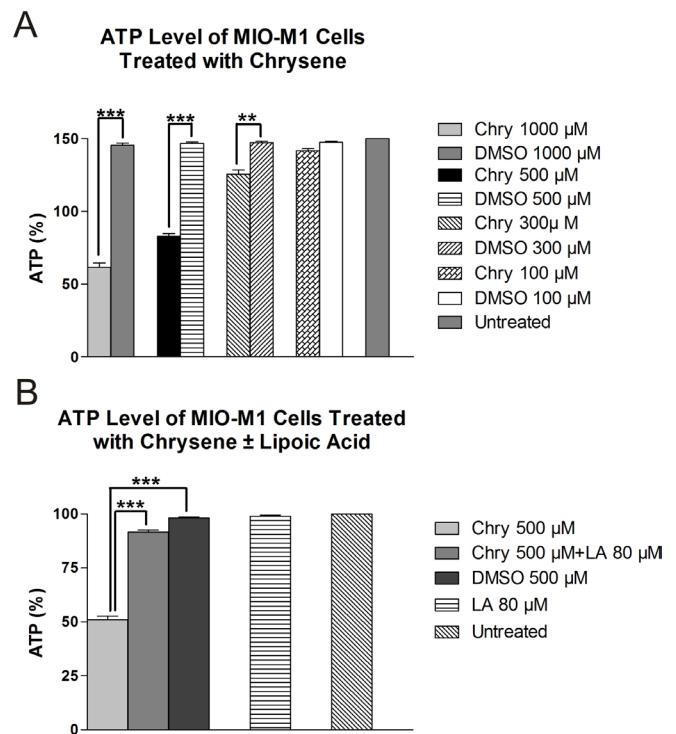


Figure 6. The effects of chrysene (Chry) on ATP production in MIO-M1 cells. **A:** The MIO-M1 cells exposed for 24 h to 1,000 μM , 500 μM , and 300 μM chrysene showed significantly lower ATP levels compared to dimethyl sulfoxide (DMSO)-equivalent-treated cells ($***p < 0.001$, $***p < 0.001$, $**p < 0.01$, respectively). The 100- μM -chrysene-treated cells had similar ATP levels to the DMSO-equivalent-treated and untreated cells. **B:** Pretreatment for 6 h with 80 μM lipaic acid (LA) significantly reversed the decline in ATP production caused by treatment with 500 μM chrysene ($***p < 0.001$). The untreated cells, DMSO-equivalent-treated cells, and 80- μM -LA-treated cells had similar ATP production levels. The assays for each concentration were run in triplicate and the experiments repeated three times. Values are mean \pm standard error mean (SEM).

both quantitative and qualitative, on the overall functioning of the macula.

Müller cells have additional functions after retinal degeneration [47,48], including re-entering the cell cycle and producing neuroprotective growth factors. Once these cells are activated, they become involved in the formation of glial scars, which occurs in late phases of retinal degeneration [47]. The proliferation of Müller cells depends on the activation of the Wnt/ β -catenin (Wnt) pathway and the sonic hedgehog (Shh) pathway [49]. The scar tissues seen clinically in some of the end stages of wet AMD are a direct result of this Müller cell activity.

We first investigated the effect of low concentrations of chrysene (20, 30, 40, and 80 μM) on the CV of MIO-M1 cells

after 24 h of exposure. Chrysene had no apparent effect on CV at these concentrations. However, there was a significant loss of CV after 7 days (chronic) treatment with 30 μ M chrysene. This damaging effect on cells demonstrates that chrysene is toxic to MIO-M1 cells and could be a contributing factor to MIO-M1 cell degeneration due to cigarette smoking. MIO-M1 cells after 24 h of treatment with 1,000, 500, and 300 μ M chrysene showed a significant concentration-dependent loss of CV as compared to their respective control. This kind of toxicity has also been shown in other cell types treated with other components found in cigarette smoke. Patil et al. have shown a significant decrease in CV in HMVEC and rat neurosensory retinal (R28) cells treated with 10^{-2} M nicotine [26]. The HMVEC cultures underwent nonapoptotic loss of cell viability and the R28 cells had decreased viability through an oxidative, noncaspase-dependent, apoptotic pathway [26]. In another study, the RPE cells were damaged through oxidative and mitochondrial dysfunction pathways after exposure to acrolein [27]. Another toxin, B(e)P, caused a dose-dependent decrease in the CV of ARPE-19 cells [24]. Both chrysene and B(e)P are PAHs, but B(e)P has five fused benzene rings, while chrysene has four fused benzene rings. Therefore, it is not surprising that both compounds would have damaging effects on cultured cells.

In the present work we elaborated on the mechanism of toxicity on MIO-M1 cells after treatment with 1,000, 500, and 300 μ M chrysene. MIO-M1 cells treated with these concentrations of chrysene for 24 h had significantly increased caspase-3/7 activity. DNA fragmentation analysis with 500 μ M chrysene also showed DNA banding that laddered in approximately 200-bp increments. Both assays are consistent with apoptosis as the mechanism of cell death. Necrosis also played a role in cell death but only at the highest concentration of chrysene (1,000 μ M). Therefore, in this system both apoptosis and necrosis might be the major mechanisms of cell death. In other assays, MIO-M1 cells treated for 24 h with 1,000, 500, and 300 μ M chrysene showed significantly increased ROS/RNS and decreased $\Delta\Psi_m$ and ATP levels, suggesting involvement of oxidative stress and mitochondrial dysfunction in chrysene-induced toxicity. Mitochondria are the main generation site of oxidants and are also a target of oxidants [50]. The constant generation of superoxide and hydroxyl radicals by mitochondria causes continuous oxidative stress. Free radicals produced during oxidative metabolism [51] can damage mitochondrial DNA (mtDNA) [52] and may increase exponentially with age. As mtDNA damage accumulates, the electron transport chain is less efficient, leading to greater free radical (superoxide) production [53]. The vicious cycle of oxidation, depletion of cellular antioxidants, such as glutathione [54], and exacerbation

of mitochondrial damage may be responsible, in part, for cellular decay. With our data we speculate that damage to the mitochondria could be the initiating event in the cascade leading to eventual apoptotic or necrotic death.

Several studies have reported on caspase activation, necrosis, oxidative stress, and mitochondrial dysfunction as a cell-death mechanism. Human RPE cells after treatment with B(e)P underwent apoptosis as shown by elevated activities of caspase-3/7, caspase-8, caspase-9, and caspase-12 [24]. Müller cells following treatment with indocyanine green dye showed that cell death and morphological changes were concentration and time dependent [55]. Human monocytic leukemia U937 cells after treatment with 2-tert-butyl-4-hydroquinone (a phenolic antioxidant used as a food additive) and 2-tert-butyl-1,4-benzoquinone (its metabolite) showed apoptotic and necrotic effects as demonstrated by elevated caspase activities, DNA fragmentation, decreased ATP, and elevated LDH levels [56]. Renal epithelial cells after exposure to iodoacetamide (a prototypical alkylating agent) showed apoptosis and necrosis [57]. Human endothelial cells and monocytes exposed to tobacco smoke and benzo[a]pyrene smoke rapidly induced complex oxidant-mediated stress responses, loss of mitochondrial membrane potential, and apoptosis or necrosis at higher concentrations that caused cell death [58]. In another report, Müller cells treated with methanol showed toxicity by ATP depletion [59]. These studies indicate that the mode of cell death differs depending on the toxin used.

Besides exploring the toxic effects of chrysene on MIO-M1 cells, we have also studied the reversal of chrysene-induced toxicity using LA. In some published reports from our laboratory, pretreatment of retinal cells with different inhibitors before exposure to toxins have shown protective effect on cells. For example, pretreatment of ARPE-19 cells with memantine, resveratrol, and genistein significantly inhibited loss of CV after exposure to B(e)P. However, ARPE-19 cells pretreated with epicatechin did not significantly reverse CV [25]. In other studies using R28 cell cultures, increased caspase-3 activity caused by 7-ketocholesterol (toxic element from oxidized low-density lipoproteins) was significantly reduced after pretreatment with epicatechin [28]. The diversity and disparity in the protection of retinal cells may be due to the nature of the toxin and type of cell lines.

MIO-M1 cultures pretreated with 80 μ M LA showed reversal of caspase-3/7, ROS/RNS, $\Delta\Psi_m$, and ATP effects induced by chrysene. This finding strongly suggests that LA offers protection to cells against caspase-dependent oxidative stress and mitochondrial dysfunction. LA is a natural metabolic antioxidant [60] that is easily absorbed, crosses the blood-brain barrier, and reaches peak levels in the central

nervous system, retina, and peripheral nerves within 0.5 h of oral administration [61]. Inside the mitochondria of the cells, mitochondrial α -keto acid dehydrogenase complexes [61] reduce LA into another more potent antioxidant—dihydrolipoate. Both LA and especially dihydrolipoate regenerate other antioxidants, such as vitamin C and vitamin E, through redox cycling and raise intracellular glutathione levels [61]. LA administration increases intracellular glutathione levels by 30–70% in cell culture and in vivo studies [62,63]. LA targets mitochondria, protects mitochondria from oxidative damage, and improves mitochondrial function. The mechanism of protection includes preventing the generation of oxidants, scavenging free radicals and iron chelating [64], inhibiting oxidant reactivity, elevating cofactors of defective mitochondria to enhance antioxidant defense system [65], and protecting enzymes from further oxidation. LA repairs oxidative damage to lipids and proteins/enzymes through activation of the phase 2 enzyme system and increases mitochondrial biogenesis and improves its function [51].

LA is available as a food supplement in grocery stores in Europe and the USA. LA is clinically safe and is considered to have a beneficial effect in several disorders, such as cerebral ischemia–reperfusion, excitotoxic amino acid brain injury, mitochondrial dysfunction, diabetes and diabetic neuropathy, inborn errors of metabolism, and other causes of acute or chronic damage to brain or neural tissue [61]. Several studies using cell culture and disease models in animals have shown favorable effects of LA. LA added to cultural rat hippocampal neurons reversed cell damage induced by glutamate [66]. Pretreatment of human fetal retinal pigment epithelial cells with LA blocked the ROS production and apoptosis and increased the mitochondrial membrane potential due to a chemical oxidant, *tert*-butylhydroperoxide [67]. Treatment with LA, creatine, nicotinamide, and epigallocatechin gallate protected ganglion cell death due to apoptosis, oxidative stress, and mitochondrial dysfunction in rats [68]. Treatment with thiocetic acid and dihydrolipoic acid demonstrated neuroprotection against N-Methyl-D-aspartic acid (NMDA) and malonic acid lesions of striatum in rats [69]. LA showed caspase-dependent and -independent inhibition of cell death against pilocarpine-induced seizures in rats [70]. LA demonstrated anti-apoptotic and neuroprotective effects on spinal cord ischemia–reperfusion in rabbits [71]. LA showed protective effects in D-galactose-induced memory loss, neurodegeneration, and oxidative damage in mice [72].

Administration of LA with other agents has shown synergistic effects in animals as well as in patients with Alzheimer disease (AD). Co-administration of LA and vitamin C inhibited oxidative stress in rats exposed to chronic

arsenic toxicity [73]. LA given with vitamin E has shown additive effects against lipid peroxidation in several pathological models for neurologic functions, glial reactivity, and neuronal remodeling in rats [74]. Administration of LA and N-acetyl cysteine has shown decreased mitochondrial-related oxidative stress in fibroblasts from AD patients [75]. It has been suggested that combined therapy of LA with antioxidants could greatly diminish the progression of AD disease [76,77]. Reports from 43 patients that were observed for 48 months provided supportive findings that LA treatment could provide neuroprotection for AD patients [78].

LA has been shown to be beneficial in some eye disorders and diabetes models. Long-term administration of LA inhibited diabetic retinopathy by reversing mitochondrial dysfunction and retinal capillary cell death in rat [79,80]. The combination of LA with lutein, zeaxanthin, and l-glutathione protected photoreceptor degeneration in animal models for retinitis pigmentosa [81]. LA, acetyl-L-carnitine, nicotinamide, and biotin have been found to improve immune dysfunction in type 2 diabetic rats [82]. The numerous reports detailed above are consistent with our findings that LA can be protective against chrysene-induced toxicity in MIO-M1 cells.

In summary, based upon our data we suggest that the mechanism of cell death of MIO-M1 cells after chrysene treatment involves both apoptosis and necrosis. Lipoic acid, a natural antioxidant, could reverse chrysene-induced apoptosis, oxidative damage, and improve mitochondrial function in Müller cells. Therefore, administering LA and its derivatives to aged people may be an effective strategy for improving or delaying neurodegenerative disorders, such as AMD.

ACKNOWLEDGMENTS

Supported by the Discovery Eye Foundation, the Henry L. Guenther Foundation, the Iris and B. Gerald Cantor Foundation, Polly and Michael Smith Foundation, the Lincy Foundation, and an unrestricted grant from Research to Prevent Blindness Foundation. We wish to thank Shari R. Atilano (Gavin Herbert Eye Institute, School of Medicine, University of California, Irvine, CA) for her preparation of figures and review of the manuscript.

REFERENCES

1. Bressler NM, Bressler SB, Fine SL. Age-related macular degeneration. *Surv Ophthalmol* 1988; 32:375-413. [PMID: 2457955].

2. Smeeth L, Cook C, Chakravarthy U, Hubbard R, Fletcher AE. A case control study of age related macular degeneration and use of statins. *Br J Ophthalmol* 2005; 89:1171-5. [PMID: 16113375].
3. DeAngelis MM, Ji F, Kim IK, Adams S, Capone A Jr, Ott J, Miller JW, Dryja TP. Cigarette smoking, CFH, APOE, ELOVL4, and risk of neovascular age-related macular degeneration. *Arch Ophthalmol* 2007; 125:49-54. [PMID: 17210851].
4. Thornton J, Edwards R, Mitchell P, Harrison RA, Buchan I, Kelly SP. Smoking and age-related macular degeneration: a review of association. *Eye (Lond)* 2005; 19:935-44. [PMID: 16151432].
5. Ni Dhubhghaill SS, Cahill MT, Campbell M, Cassidy L, Humphries MM, Humphries P. The pathophysiology of cigarette smoking and age-related macular degeneration. *Adv Exp Med Biol* 2010; 664:437-46. [PMID: 20238045].
6. Chakravarthy U, Augood C, Bentham GC, de Jong PT, Rahu M, Seland J, Soubrane G, Tomazzoli L, Topouzis F, Vingerling JR. Cigarette smoking and age-related macular degeneration in the EUREYE Study. *Ophthalmology* 2007; 114:1157-63. [PMID: 17337063].
7. Recurrent choroidal neovascularization after argon laser photocoagulation for neovascular maculopathy. *Macular Photocoagulation Study Group. Arch Ophthalmol* 1986; 104:503-12. [PMID: 2420315].
8. Khan JC, Thurlby DA, Shahid H, Clayton DG, Yates JR, Bradley M, Moore AT, Bird AC. Smoking and age related macular degeneration. the number of pack years of cigarette smoking is a major determinant of risk for both geographic atrophy and choroidal neovascularisation. *Br J Ophthalmol* 2006; 90:75-80. [PMID: 16361672].
9. Hecht SS, Bondinell WE, Hoffmann D. Chrysene and methylchrysenes. presence in tobacco smoke and carcinogenicity. *J Natl Cancer Inst* 1974; 53:1121-33. [PMID: 4427391].
10. Doong RA, Lin YT. Characterization and distribution of polycyclic aromatic hydrocarbon contaminations in surface sediment and water from Gao-ping River, Taiwan. *Water Res* 2004; 38:1733-44. [PMID: 15026227].
11. Saha M, Togo A, Mizukawa K, Murakami M, Takada H, Zakaria MP, Chiem NH, Tuyen BC, Prudente M, Boonyatumanond R, Sarkar SK, Bhattacharya B, Mishra P, Tana TS. Sources of sedimentary PAHs in tropical Asian waters: differentiation between pyrogenic and petrogenic sources by alkyl homolog abundance. *Mar Pollut Bull* 2009; 58:189-200. [PMID: 19117577].
12. Falahatpisheh M, Kerzee J, Metz R, Donnelly K, Ramos K. Inducible cytochrome P450 activities in renal glomerular mesangial cells: biochemical basis for antagonistic interactions among nephrocarcinogenic polycyclic aromatic hydrocarbons. *J Carcinog* 2004; 3:12-[PMID: 15315710].
13. Vakharia DD, Liu N, Pause R, Fasco M, Bessette E, Zhang QY, Kaminsky LS. Polycyclic aromatic hydrocarbon/metal mixtures: effect on PAH induction of CYP1A1 in human HEPG2 cells. *Drug Metab Dispos* 2001; 29:999-1006. [PMID: 11408366].
14. Heidel SM, MacWilliams PS, Baird WM, Dashwood WM, Buters JT, Gonzalez FJ, Larsen MC, Czuprynski CJ, Jefcoate CR. Cytochrome P4501B1 mediates induction of bone marrow cytotoxicity and preleukemia cells in mice treated with 7,12-dimethylbenz[a]anthracene. *Cancer Res* 2000; 60:3454-60. [PMID: 10910056].
15. Cheung YL, Gray TJ, Ioannides C. Mutagenicity of chrysene, its methyl and benzo derivatives, and their interactions with cytochromes P-450 and the Ah-receptor; relevance to their carcinogenic potency. *Toxicology* 1993; 81:69-86. [PMID: 8396278].
16. Hoffmann D, Bondinell WE, Wynder EL. Carcinogenicity of methylchrysenes. *Science* 1974; 183:215-6. [PMID: 4808861].
17. Mahadevan B, Luch A, Atkin J, Nguyen T, Sharma AK, Amin S, Baird WM. Investigation of the genotoxicity of dibenzo[c,p]chrysene in human carcinoma MCF-7 cells in culture. *Chem Biol Interact* 2006; 164:181-91. [PMID: 17094953].
18. Peden-Adams MM, Liu J, Knutson S, Dancik J, Bryant K, Bodine AB, Dickerson RL. Alterations in immune function and CYP450 activity in adult male deer mice (*Peromyscus maniculatus*) following exposure to benzo[a]pyrene, pyrene, or chrysene. *J Toxicol Environ Health A* 2007; 70:1783-91. [PMID: 17934950].
19. Machala M, Svihalkova-Sindlerova L, Pencikova K, Kremer P, Topinka J, Milcova A, Novakova Z, Kozubik A, Vondracek J. Effects of methylated chrysenes on AhR-dependent and -independent toxic events in rat liver epithelial cells. *Toxicology* 2008; 247:93-101. [PMID: 18407395].
20. Karacik B, Okay OS, Henkelmann B, Bernhoft S, Schramm KW. Polycyclic aromatic hydrocarbons and effects on marine organisms in the Istanbul Strait. *Environ Int* 2009; 35:599-606. [PMID: 19128832].
21. Green WR, McDonnell PJ, Yeo JH. Pathologic features of senile macular degeneration. 1985. *Retina* 2005; 25:Suppl615-27. [PMID: 16049365].
22. Spraul CW, Lang GE, Lang GK, Grossniklaus HE. Morphometric changes of the choriocapillaris and the choroidal vasculature in eyes with advanced glaucomatous changes. *Vision Res* 2002; 42:923-32. [PMID: 11927356].
23. Dunaief JL, Dentchev T, Ying GS, Milam AH. The role of apoptosis in age-related macular degeneration. *Arch Ophthalmol* 2002; 120:1435-42. [PMID: 12427055].
24. Sharma A, Neekhara A, Gramajo AL, Patil J, Chwa M, Kuppermann BD, Kenney MC. Effects of Benzo(e)Pyrene, a toxic component of cigarette smoke, on human retinal pigment epithelial cells in vitro. *Invest Ophthalmol Vis Sci* 2008; 49:5111-7. [PMID: 18586875].
25. Mansoor S, Gupta N, Patil AJ, Estrago-Franco MF, Ramirez C, Migon R, Sapkal A, Kuppermann BD, Kenney MC. Inhibition of apoptosis in human retinal pigment epithelial cells

- treated with benzo(e)pyrene, a toxic component of cigarette smoke. *Invest Ophthalmol Vis Sci* 2010; 51:2601-7. [PMID: 19959636].
26. Patil AJ, Gramajo AL, Sharma A, Seigel GM, Kuppermann BD, Kenney MC. Differential effects of nicotine on retinal and vascular cells in vitro. *Toxicology* 2009; 259:69-76. [PMID: 19428945].
 27. Jia L, Liu Z, Sun L, Miller SS, Ames BN, Cotman CW, Liu J. Acrolein, a toxicant in cigarette smoke, causes oxidative damage and mitochondrial dysfunction in RPE cells: protection by (R)-alpha-lipoic acid. *Invest Ophthalmol Vis Sci* 2007; 48:339-48. [PMID: 17197552].
 28. Neekhra A, Luthra S, Chwa M, Seigel G, Gramajo AL, Kuppermann BD, Kenney MC. Caspase-8, -12, and -3 activation by 7-ketocholesterol in retinal neurosensory cells. *Invest Ophthalmol Vis Sci* 2007; 48:1362-7. [PMID: 17325185].
 29. Derin N, Akpınar D, Yargıoğlu P, Agar A, Aslan M. Effect of alpha-lipoic acid on visual evoked potentials in rats exposed to sulfite. *Neurotoxicol Teratol* 2009; 31:34-9. [PMID: 18761084].
 30. Freitas RM. The evaluation of effects of lipoic acid on the lipid peroxidation, nitrite formation and antioxidant enzymes in the hippocampus of rats after pilocarpine-induced seizures. *Neurosci Lett* 2009; 455:140-4. [PMID: 19368863].
 31. Li L, Holian A. Acrolein: a respiratory toxin that suppresses pulmonary host defense. *Rev Environ Health* 1998; 13:99-108. [PMID: 9718625].
 32. Moini H, Packer L, Saris NE. Antioxidant and prooxidant activities of alpha-lipoic acid and dihydrolipoic acid. *Toxicol Appl Pharmacol* 2002; 182:84-90. [PMID: 12127266].
 33. Kamenova P. Improvement of insulin sensitivity in patients with type 2 diabetes mellitus after oral administration of alpha-lipoic acid. *Hormones (Athens)* 2006; 5:251-8. [PMID: 17178700].
 34. Liu J, Ames BN. Reducing mitochondrial decay with mitochondrial nutrients to delay and treat cognitive dysfunction, Alzheimer's disease, and Parkinson's disease. *Nutr Neurosci* 2005; 8:67-89. [PMID: 16053240].
 35. Evans JL, Goldfine ID. Alpha-lipoic acid: a multifunctional antioxidant that improves insulin sensitivity in patients with type 2 diabetes. *Diabetes Technol Ther* 2000; 2:401-13. [PMID: 11467343].
 36. Limb GA, Salt TE, Munro PM, Moss SE, Khaw PT. In vitro characterization of a spontaneously immortalized human Muller cell line (MIO-M1). *Invest Ophthalmol Vis Sci* 2002; 43:864-9. [PMID: 11867609].
 37. Narayanan R, Kenney MC, Kamjoo S, Trinh TH, Seigel GM, Resende GP, Kuppermann BD. Trypan blue: effect on retinal pigment epithelial and neurosensory retinal cells. *Invest Ophthalmol Vis Sci* 2005; 46:304-9. [PMID: 15623789].
 38. Chwa M, Atilano SR, Reddy V, Jordan N, Kim DW, Kenney MC. Increased stress-induced generation of reactive oxygen species and apoptosis in human keratoconus fibroblasts. *Invest Ophthalmol Vis Sci* 2006; 47:1902-10. [PMID: 16638997].
 39. Zarbin MA. Current concepts in the pathogenesis of age-related macular degeneration. *Arch Ophthalmol* 2004; 122:598-614. [PMID: 15078679].
 40. Newman E, Reichenbach A. The Muller cell: a functional element of the retina. *Trends Neurosci* 1996; 19:307-12. [PMID: 8843598].
 41. Constable PA, Lawrenson JG. Glial cell factors and the outer blood retinal barrier. *Ophthalmic Physiol Opt* 2009; 29:557-64. [PMID: 19689550].
 42. Combadière C, Feumi C, Raoul W, Keller N, Rodéro M, Pézard A, Lavalette S, Houssier M, Jonet L, Picard E, Debré P, Sirinyan M, Deterre P, Ferroukhi T, Cohen SY, Chauvaud D, Jeanny JC, Chemtob S, Behar-Cohen F, Sennlaub F. CX3CR1-dependent subretinal microglia cell accumulation is associated with cardinal features of age-related macular degeneration. *J Clin Invest* 2007; 117:2920-8. [PMID: 17909628].
 43. Das AV, Mallya KB, Zhao X, Ahmad F, Bhattacharya S, Thoreson WB, Hegde GV, Ahmad I. Neural stem cell properties of Muller glia in the mammalian retina: regulation by Notch and Wnt signaling. *Dev Biol* 2006; 299:283-302. [PMID: 16949068].
 44. Kubota A, Nishida K, Nakashima K, Tano Y. Conversion of mammalian Muller glial cells into a neuronal lineage by in vitro aggregate-culture. *Biochem Biophys Res Commun* 2006; 351:514-20. [PMID: 17070773].
 45. Osakada F, Ooto S, Akagi T, Mandai M, Akaike A, Takahashi M. Wnt signaling promotes regeneration in the retina of adult mammals. *J Neurosci* 2007; 27:4210-9. [PMID: 17428999].
 46. Ooto S. Potential for neural regeneration in the adult mammalian retina. *Nippon Ganka Gakkai Zasshi* 2006; 110:864-71. [PMID: 17134034].
 47. Bringmann A, Pannicke T, Grosche J, Francke M, Wiedemann P, Skatchkov SN, Osborne NN, Reichenbach A. Muller cells in the healthy and diseased retina. *Prog Retin Eye Res* 2006; 25:397-424. [PMID: 16839797].
 48. Burke JM, Smith JM. Retinal proliferation in response to vitreous hemoglobin or iron. *Invest Ophthalmol Vis Sci* 1981; 20:582-92. [PMID: 7216676].
 49. Wan J, Zheng H, Xiao HL, She ZJ, Zhou GM. Sonic hedgehog promotes stem-cell potential of Muller glia in the mammalian retina. *Biochem Biophys Res Commun* 2007; 363:347-54. [PMID: 17880919].
 50. Shigenaga MK, Hagen TM, Ames BN. Oxidative damage and mitochondrial decay in aging. *Proc Natl Acad Sci USA* 1994; 91:10771-8. [PMID: 7971961].
 51. Nohl H, Jordan W. The mitochondrial site of superoxide formation. *Biochem Biophys Res Commun* 1986; 138:533-9. [PMID: 3017331].
 52. Richter C, Park JW, Ames BN. Normal oxidative damage to mitochondrial and nuclear DNA is extensive. *Proc Natl Acad Sci USA* 1988; 85:6465-7. [PMID: 3413108].

53. Saggiu H, Cooksey J, Dexter D, Wells FR, Lees A, Jenner P, Marsden CD. A selective increase in particulate superoxide dismutase activity in parkinsonian substantia nigra. *J Neurochem* 1989; 53:692-7. [PMID: 2760616].
54. Tritschler HJ, Packer L, Medori R. Oxidative stress and mitochondrial dysfunction in neurodegeneration. *Biochem Mol Biol Int* 1994; 34:169-81. [PMID: 7849618].
55. Matsui H, Karasawa Y, Sato T, Kanno S, Nishikawa S, Okisaka S. Toxicity of indocyanine green dye on Müller cells. *Nippon Ganka Gakkai Zasshi* 2007; 111:587-93. [PMID: 17874533].
56. Okubo T, Yokoyama Y, Kano K, Kano I. Cell death induced by the phenolic antioxidant tert-butylhydroquinone and its metabolite tert-butylquinone in human monocytic leukemia U937 cells. *Food Chem Toxicol* 2003; 41:679-88. [PMID: 12659721].
57. van De Water B, Wang Y, Asmellash S, Liu H, Zhan Y, Miller E, Stevens JL. Distinct endoplasmic reticulum signaling pathways regulate apoptotic and necrotic cell death following iodoacetamide treatment. *Chem Res Toxicol* 1999; 12:943-51. [PMID: 10525270].
58. Vayssier-Taussat M, Camilli T, Aron Y, Meplan C, Hainaut P, Polla BS, Weksler B. Effects of tobacco smoke and benzo[a]pyrene on human endothelial cell and monocyte stress responses. *Am J Physiol Heart Circ Physiol* 2001; 280:H1293-300. [PMID: 11179076].
59. Garner CD, Lee EW, Louis-Ferdinand RT. Müller cell involvement in methanol-induced retinal toxicity. *Toxicol Appl Pharmacol* 1995; 130:101-7. [PMID: 7839358].
60. Reed LJ, De BB, Gunsalus IC, Hornberger CS Jr. Crystalline alpha-lipoic acid; a catalytic agent associated with pyruvate dehydrogenase. *Science* 1951; 114:93-4. [PMID: 14854913].
61. Packer L, Tritschler HJ, Wessel K. Neuroprotection by the metabolic antioxidant alpha-lipoic acid. *Free Radic Biol Med* 1997; 22:359-78. [PMID: 8958163].
62. Busse E, Zimmer G, Schopohl B, Kornhuber B. Influence of alpha-lipoic acid on intracellular glutathione in vitro and in vivo. *Arzneimittelforschung* 1992; 42:829-31. [PMID: 1418040].
63. Han D, Tritschler HJ, Packer L. Alpha-lipoic acid increases intracellular glutathione in a human T-lymphocyte Jurkat cell line. *Biochem Biophys Res Commun* 1995; 207:258-64. [PMID: 7857274].
64. Ou P, Tritschler HJ, Wolff SP. Thioctic (lipoic) acid: a therapeutic metal-chelating antioxidant? *Biochem Pharmacol* 1995; 50:123-6. [PMID: 7605337].
65. Packer L, Witt EH, Tritschler HJ. alpha-Lipoic acid as a biological antioxidant. *Free Radic Biol Med* 1995; 19:227-50. [PMID: 7649494].
66. Müller U, Krieglstein J. Prolonged pretreatment with alpha-lipoic acid protects cultured neurons against hypoxic, glutamate-, or iron-induced injury. *J Cereb Blood Flow Metab* 1995; 15:624-30. [PMID: 7790411].
67. Voloboueva LA, Liu J, Suh JH, Ames BN, Miller SS. (R)-alpha-lipoic acid protects retinal pigment epithelial cells from oxidative damage. *Invest Ophthalmol Vis Sci* 2005; 46:4302-10. [PMID: 16249512].
68. Osborne NN. Pathogenesis of ganglion "cell death" in glaucoma and neuroprotection: focus on ganglion cell axonal mitochondria. *Prog Brain Res* 2008; 173:339-52. [PMID: 18929120].
69. Greenamyre JT, Garcia-Osuna M, Greene JG. The endogenous cofactors, thioctic acid and dihydrolipoic acid, are neuroprotective against NMDA and malonic acid lesions of striatum. *Neurosci Lett* 1994; 171:17-20. [PMID: 8084483].
70. dos Santos PS, Feitosa CM, Saldanha GB, Tomé Ada R, Feng D, de Freitas RM. Lipoic acid inhibits caspase-dependent and -independent cell death pathways and is neuroprotective against hippocampal damage after pilocarpine-induced seizures. *Pharmacol Biochem Behav* 2011; 97:531-6. [PMID: 21062633].
71. Emmez H, Yildirim Z, Kale A, Töngge M, Durdağ E, Börcek AO, Uçankuş LN, Doğulu F, Kiliç N, Baykaner MK. Anti-apoptotic and neuroprotective effects of alpha-lipoic acid on spinal cord ischemia-reperfusion injury in rabbits. *Acta Neurochir (Wien)* 2010; 152:1591-600. [PMID: 20535507].
72. Cui X, Zuo P, Zhang Q, Li X, Hu Y, Long J, Packer L, Liu J. Chronic systemic D-galactose exposure induces memory loss, neurodegeneration, and oxidative damage in mice: protective effects of R-alpha-lipoic acid. *J Neurosci Res* 2006; 83:1584-90. [PMID: 16555301].
73. Liu CB, Feng YH, Ye GH, Xiao M. Effects of alpha-lipoic acid and vitamin C on oxidative stress in rat exposed to chronic arsenic toxicity. *Zhonghua Lao Dong Wei Sheng Zhi Ye Bing Za Zhi* 2010; 28:891-4. [PMID: 21241596].
74. Gonzalez-Perez O, Gonzalez-Castaneda RE, Huerta M, Luquin S, Gomez-Pinedo U, Sanchez-Almaraz E, Navarro-Ruiz A, Garcia-Estrada J. Beneficial effects of alpha-lipoic acid plus vitamin E on neurological deficit, reactive gliosis and neuronal remodeling in the penumbra of the ischemic rat brain. *Neurosci Lett* 2002; 321:100-4. [PMID: 11872266].
75. Moreira PI, Harris PL, Zhu X, Santos MS, Oliveira CR, Smith MA, Perry G. Lipoic acid and N-acetyl cysteine decrease mitochondrial-related oxidative stress in Alzheimer disease patient fibroblasts. *J Alzheimers Dis* 2007; 12:195-206. [PMID: 17917164].
76. Maczurek A, Hager K, Kenklies M, Sharman M, Martins R, Engel J, Carlson DA, Münch G. Lipoic acid as an anti-inflammatory and neuroprotective treatment for Alzheimer's disease. *Adv Drug Deliv Rev* 2008; 60:1463-70. [PMID: 18655815].
77. Holmquist L, Stuchbury G, Berbaum K, Muscat S, Young S, Hager K, Engel J, Münch G. Lipoic acid as a novel treatment for Alzheimer's disease and related dementias. *Pharmacol Ther* 2007; 113:154-64. [PMID: 16989905].
78. Hager K, Kenklies M, McAfoose J, Engel J, Münch G. Alpha-lipoic acid as a new treatment option for Alzheimer's disease—a 48 months follow-up analysis. *J Neural Transm Suppl* 2007; 72:189-93. [PMID: 17982894].

79. Kowluru RA, Odenbach S. Effect of long-term administration of alpha-lipoic acid on retinal capillary cell death and the development of retinopathy in diabetic rats. *Diabetes* 2004; 53:3233-8. [PMID: 15561955].
80. Kowluru RA. Diabetic retinopathy: mitochondrial dysfunction and retinal capillary cell death. *Antioxid Redox Signal* 2005; 7:1581-7. [PMID: 16356121].
81. Sanz MM, Johnson LE, Ahuja S, Ekström PA, Romero J, van Veen T. Significant photoreceptor rescue by treatment with a combination of antioxidants in an animal model for retinal degeneration. *Neuroscience* 2007; 145:1120-9. [PMID: 17293057].
82. Hao J, Shen W, Tian C, Liu Z, Ren J, Luo C, Long J, Sharman E, Liu J. Mitochondrial nutrients improve immune dysfunction in the type 2 diabetic Goto-Kakizaki rats. *J Cell Mol Med* 2009; 13:701-11. [PMID: 18410524].

Articles are provided courtesy of Emory University and the Zhongshan Ophthalmic Center, Sun Yat-sen University, P.R. China. The print version of this article was created on 7 January 2013. This reflects all typographical corrections and errata to the article through that date. Details of any changes may be found in the online version of the article.